Chemical Engineering Journal 356 (2019) 393–399

Contents lists available at ScienceDirect

Chemical Engineering Journal

journal homepage: www.elsevier.com/locate/cej

Robust photocatalytic reduction of Cr(VI) on UiO-66-NH_2(Zr/Hf) metal-organic framework membrane under sunlight irradiation

Xue-Dong Du[a], Xiao-Hong Yi[a], Peng Wang[a], Weiwei Zheng[b], Jiguang Deng[c,*], Chong-Chen Wang[a,*]

[a] Beijing Key Laboratory of Functional Materials for Building Structure and Environment Remediation, Beijing University of Civil Engineering and Architecture, Beijing 100044, China
[b] Department of Chemistry, Syracuse University, Syracuse, NY 13244, United States
[c] Department of Chemistry and Chemical Engineering, College of Environmental and Energy Engineering, Beijing University of Technology, Beijing 100124, China

HIGHLIGHTS

- The UiO-66-NH_2 membranes were grown on the α-Al_2O_3 substrate.
- The membranes exhibited good photocatalytic Cr(VI) activities under sunlight.
- Foreign ions exposed no adverse effects to their photocatalytic activities.
- The UiO-66-NH_2(Zr/Hf) membranes possessed good recyclability and stability.

GRAPHICAL ABSTRACT

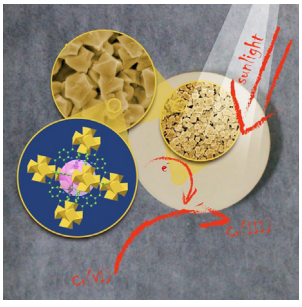

ARTICLE INFO

Keywords:
UiO-66-NH_2(Zr/Hf)
MOF membrane
Photocatalysis
Cr(VI) reduction
Sunlight

ABSTRACT

The removal of toxic hexavalent chromium (Cr(VI)) ions from surface and ground water is highly demanded. While photocatalytic reduction of Cr(VI) to Cr(III) by traditional powder photocatalysts is a promising method, the difficult in the separation of the photocatalysts from the water hinders their wide practical applications. Herein we present the use of metal-organic framework (MOF) UiO-66-NH_2(Zr/Hf) membrane as photocatalysts to reduce Cr(VI) ions with high efficiency and easy separation from the treated waste water. The UiO-66-NH_2(Zr/Hf) MOF membrane photocatalysts were fabricated via a reactive seeding method on a α-Al_2O_3 substrate. It was found that the UiO-66-NH_2(Zr/Hf) membranes exhibited excellent photocatalytic Cr(VI) reduction performance under both simulated and real sunlight irradiation. The UiO-66-NH_2(Zr) membrane can maintain more than 94% Cr(VI) reduction efficiency after 20 cycles because of its exceptional chemical and water stability. The influences of foreign ions on Cr(VI) reduction were investigated to mimic real lake water, which revealed that no obvious adverse effects can be found with the presence of common foreign ions in surface water. The MOF membrane photocatalysts provide a new approach to carry out efficiently photocatalytic removal of pollutants in wastewater.

* Corresponding authors.
E-mail addresses: jgdeng@bjut.edu.cn (J. Deng), wangchongchen@bucea.edu.cn (C.-C. Wang).

https://doi.org/10.1016/j.cej.2018.09.084
Received 24 July 2018; Received in revised form 7 September 2018; Accepted 10 September 2018
Available online 11 September 2018
1385-8947/

1. Introduction

Among toxic heavy metal ions, hexavalent chromium (Cr(VI)) is a mutagenic and carcinogenic contaminant in surface and ground water, as it is widely utilized in electroplating, leather tanning, printing, polishing and pigment industries [1,2]. Up to now, many techniques such as adsorption [3], ion change [4], membrane filtration [5], and reduction from Cr(VI) to Cr(III) [6,7] have been developed to remove Cr (VI) from wastewater. The reduction from Cr(VI) to Cr(III) is highly desirable, considering Cr(III) has a lowly toxicity and easily forms insoluble precipitates such as $Cr(OH)_3$ in neutral or basic solutions [8]. Compared to traditional reduction technologies such as electro-chemical reduction, chemical reduction, and micro-reduction, photocatalytic reduction of Cr(VI) to Cr(III) has the advantages of high efficiency, low-cost, and is free of any hazardous chemical formation [6]. Various nano-sized photocatalysts, such as TiO_2, ZnO, CdS, GaP, g-C_3N_4, and *etc*. [8–12], have been used to reduce Cr(VI) into Cr(III) under UV light or visible light. Unfortunately, these photocatalysts suffered from their quick electron–hole recombination, poor reduction efficiency and slow reduction rate [13]. As the emerging photocatalysts, metal-organic framework (MOFs) were widely utilized to efficiently reduce Cr(VI) into Cr(III) using photogenerated electrons, due to their merits of desirable topologies, high surface areas along with efficient light harvest via rational modification of organic linkers (like $–NH_2$) [13–18]. For instance, UiO-66-NH_2 and its derivatives have been used to accomplish outstanding photocatalytic Cr(VI) reduction [19,20]. However, both nano-sized photocatalysts and MOFs powders are very difficult to separate from treated water for recycle, which heavily hinders their practical applications [21]. Recently, the deposition of MOFs on substrates to fabricate corresponding membranes have attracted increasing attentions for use in catalysis, sensors, and especially separations [22,23]. However, up to now, only $Zn_3(BTC)_2$ MOF membrane was fabricated on zinc plates to conduct photocatalytic degradation of methylene blue to our best knowledge [24]. In this work, UiO-66-NH_2(Zr/Hf) membranes were fabricated on an α-Al_2O_3 support by a reactive seeding method. The MOF membranes were characterized by powder X-Ray diffraction (PXRD), Fourier Transform infrared spectroscopy (FTIR), scanning electron microscopy (SEM), and UV-vis diffuse reflection spectroscopy (UV-Vis DRS). The UiO-66-NH_2(Zr/Hf) membranes demonstrated outstanding photocatalytic performance on Cr(VI) reduction under both simulated and real sunlight irradiation. The MOF membranes could be easily separated from treated solution and for further reuse, therefore exhibited great potential for the photocatalytic removal of pollutants from wastewater.

2. Experimental

2.1. Materials and characterization

All reagents and solvents were commercially available and used without further treatment. 2-Aminoterephthalic acid (H_2ATA, $C_8H_7NO_4$, 99.0%), zirconium tetrachloride ($ZrCl_4$, 98.0%), hafnium tetrachloride ($HfCl_4$, 98.0%) and 1,5-diphenylcarbazide ($C_{13}H_{14}N_4O$, 98%) were purchased from J&k Scientific Ltd. Potassium dichromate ($K_2Cr_2O_7$, guaranteed reagent), N'N-dimethylformamide (DMF, $C_5H_{13}NO_2$, analytical reagent), concentrated sulfuric acid (H_2SO_4, analytical reagent), phosphoric acid (H_3PO_4, analytical reagent), sodium hydroxide (NaOH, analytical reagent), anhydrous ethanol (CH_3CH_2OH), anhydrous acetone (CH_3COCH_3, analytical reagent), and acetic acid (HAc, CH_3COOH, analytical reagent) were purchased from Sinopharm Chemical Reagent Co., Ltd.

The PXRD patterns were recorded on a Dandonghaoyuan DX-2700B diffractometer in the range of 2θ = 5°–50° with Cu Kα radiation. The morphologies of membranes were studied by a field emission scanning electron microscopy (SEM) (SU8020, Hitachi Limited, Japan). The Fourier transform infrared (FTIR) spectra were recorded on a Nicolet 6700 spectrometer in the range of 4000–400 cm^{-1} with KBr pellets. UV-visible diffuse-reflectance spectra (UV-vis DRS) of membrane were recorded from 200 to 800 nm with a Perkin Elmer Lamda 650S spectrophotometer, in which barium sulfate ($BaSO_4$) was used as the standard with 100% reflectance. The thickness of the membrane was measured by a SE850DUV ellipsometer with the incidence angle of 70°.

2.2. Preparation of UiO-66-NH_2(Zr) membrane

Alumina support was prepared by a solid-phase reaction [25,26] between alumina powder (particle size of ~1 μm) and starch as a pore forming agent. Firstly, alumina powder and starch, with a mass ratio of 9:1, were mixed in the stainless-steel pot with the aid of a suitable amount of deionized water, and subsequently ground for 750 min to obtain slurry using a ball mill. Secondly, the slurry was heated and agitated at a high rate of speed until the water evaporated completely. Finally, alumina powder was pressed at 20 MPa to prepare disks with diameters of 25 mm and thicknesses of 3 mm. The disks were thermally treated at 1523 K for 12 h, and then cooled at rate of 274 K/min. One side of the α-Al_2O_3 support was polished with SiC sandpaper and washed in deionized water before being used for the growth of MOF membrane.

The UiO-66-NH_2(Zr) membrane was fabricated on an α-Al_2O_3 support by a modified reactive seeding (RS) method [27]. The synthesis includes two steps: (i) Seed growth: H_2ATA (2.0 mmol, 0.3623 g) was dispersed in deionized H_2O (25.0 mL) by sonication for 10 min. An α-Al_2O_3 support was placed horizontally in an 80 mL Teflon lined stainless steel autoclave with the H_2ATA aqueous solution. The autoclave was heated at 453 K for 12 h in an oven, and then cooled down to room temperature. After that, the seeded support was washed with deionized water and dried at 333 K for 6 h. (ii) Secondary growth: a mixture of $ZrCl_4$ (1.0 mmol, 0.2330 g), H_2ATA (1.0 mmol, 0.1812 g) DMF (17.0 mL) and acetic acid (7.0 mL) was sealed in an 80 mL Teflon lined stainless steel autoclave containing the seeded support. The autoclave was heated at 423 K for 48 h in the oven, and then cooled down to room temperature. Finally, the MOF membrane was washed with DMF and anhydrous ethanol, and then dried at 333 K for 6 h before further analysis. Preparation of UiO-66-NH_2(Hf) membrane followed the same procedure as the UiO-66-NH_2(Zr) membrane, except that $ZrCl_4$ (1.0 mmol, 0.2330 g) was replaced with $HfCl_4$ (1.0 mmol, 0.3203 g).

2.3. Electrochemistry measurements

The study of the electrochemical properties of UiO-66-NH_2(Zr/Hf) membranes proved difficult as the Al_2O_3 substrate provided electrical insulation. In this study, we carried out the electrochemical measurements using UiO-66-NH_2(Zr/Hf) powder samples following identical conditions to that of the membranes. To prepare the working electrodes, 5.0 mg UiO-66-NH_2(Zr) or UiO-66-NH_2(Hf) powder samples were mixed with 400.0 μL ethanol/Nafion (v/v = 19/1), which was dispersed under sonication for 30 min. 10.0 μL prepared slurry was drop-casted onto the surface of a FTO substrate (1.0 cm × 1.0 cm), and then dried in air at 353 K for 30 min. This step was repeated five times to ensure the uniform coverage of UiO-66-NH_2(Zr) or UiO-66-NH_2(Hf) samples on the FTO substrate. The electrochemical measurements were performed via a Metrohm Autolab PGSTAT204 electrochemical station in a typical three-electrode mode with 0.2 M Na_2SO_4 solution (pH = 6.8) as the electrolyte. A saturated Ag/AgCl electrode and a platinum (Pt) electrode were used as the reference electrode and counter electrode, respectively. A 300 W Xenon lamp (Beijing Aulight Co., Ltd) was used as a light source.

2.4. Photocatalytic experiment

The photocatalytic reduction of Cr(VI) into Cr(III) was carried out at room temperature in a 300 mL quartz reactor containing an as-prepared

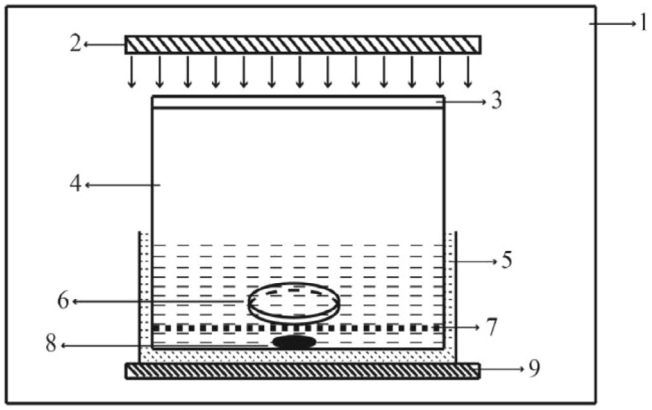

Fig. 1. Equipment setup of photocatalytic experiment: 1. Stainless steel shell; 2. Light source; 3. Quartz slices; 4. Reactor; 5. Cooling water; 6. UiO-66-NH_2 membrane; 7. Sieve plate; 8. Magnetic stirrer rotor; 9. Magnetic stirrer.

UiO-66-NH_2(Zr) membrane or UiO-66-NH_2(Hf) membrane and 30.0 mL 5.0 ppm Cr(VI) aqueous solution (Fig. 1), in which the solution pH value was adjusted to 2.0 with 0.2 M of H_2SO_4 or 0.2 M of NaOH. The solution was irradiated by a 300 W Xenon lamp (Beijing Aulight Co., Ltd), and the spectrum of light source (greater than 400 nm) was shown in Fig. S1. During illumination, about 1.2 mL of solution was taken from the reactor at certain time intervals and filtered through a 0.45 μm membrane filter. The Cr(VI) content in the supernatant solution was determined colorimetrically at 540 nm using the diphenylcarbazide method with a YuanXi UV-5200PC UV-vis spectrophotometer [28].

3. Results and discussion

3.1. Fabrication of UiO-66-NH_2(Zr/Hf) MOF membrane on α-alumina supports

In this work, a reactive seeding (RS) method was used to fabricate a thin, uniform and well intergrown UiO-66-NH_2(Zr/Hf) MOF membrane [27]. Compared with the in-situ growth method, the seeded growth method can offer better control of MOFs membrane microstructure and obtain a high coverage on supports [23]. A schematic of the fabrication of UiO-66-NH_2(Zr/Hf) membrane on the α-Al_2O_3 support via the RS method is illustrated in Fig. 2a. Firstly, a uniform seeding layer grows on the support from the reaction between H_2ATA and α-Al_2O_3 under hydrothermal conditions (453 K for 12 h) [27]. Secondly, UiO-66-NH_2(Zr) membrane or UiO-66-NH_2(Hf) membrane was fabricated from the reaction between H_2ATA and $ZrCl_4$ or $HfCl_4$ in the mixed solution of DMF and HAc (v/v = 17/7) under solvothermal conditions (423 K for 48 h) in a 25 mL Teflon-lined stainless-steel Parr bomb. The color of the surface of α-Al_2O_3 support changed from white to brown after the first step, and then becomes yellow after the second step. Compared with the surface of α-Al_2O_3, the surface morphology of the seeded layer is denser (Fig. 2b and c), implying H_2ATA has adhered to the α-Al_2O_3 support.

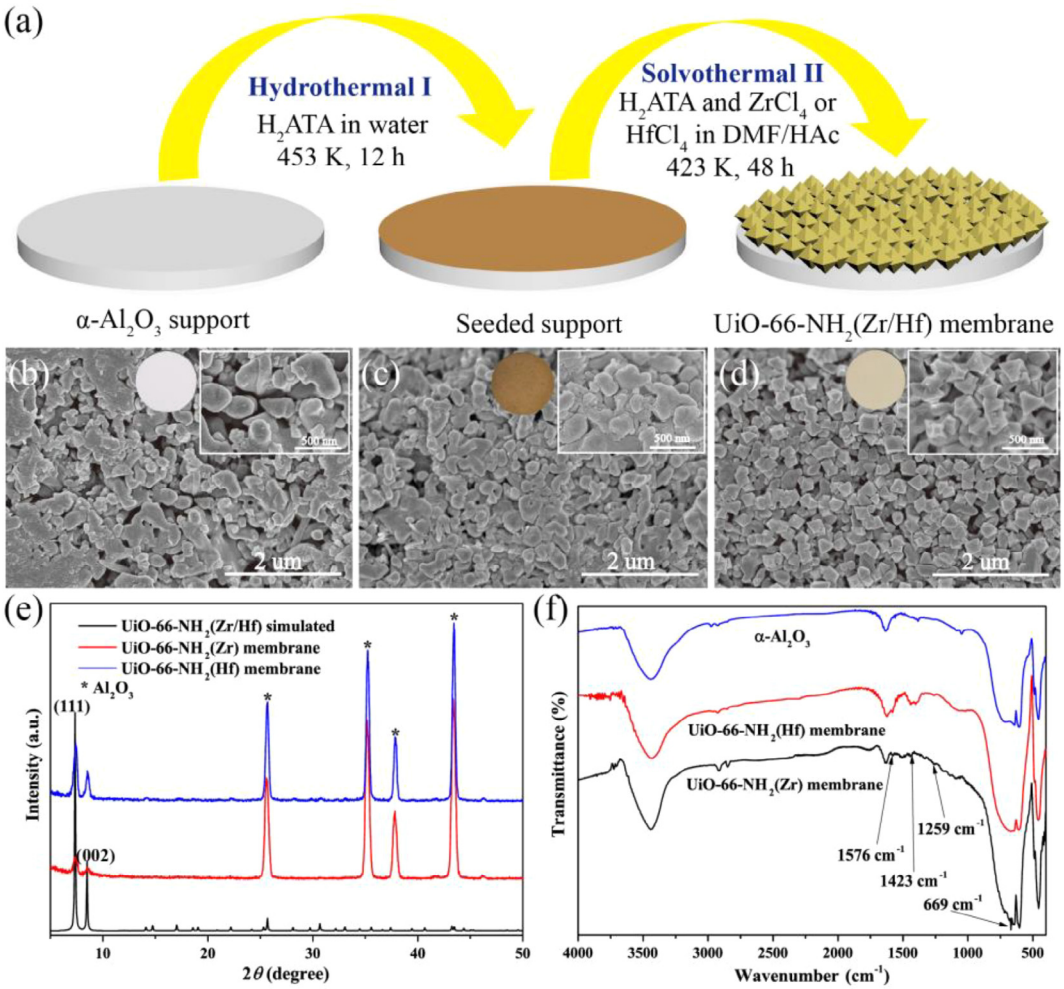

Fig. 2. (a) Schematic diagram of UiO-66-NH_2(Zr/Hf) membrane preparation procedure. SEM images of the (b) α-Al_2O_3 support, (c) seed layer, (d) UiO-66-NH_2(Zr) membrane surface. (e) XRD patterns of UiO-66-NH_2(Zr/Hf) membrane. (f) FTIR spectra of UiO-66-NH_2(Zr/Hf) membrane.

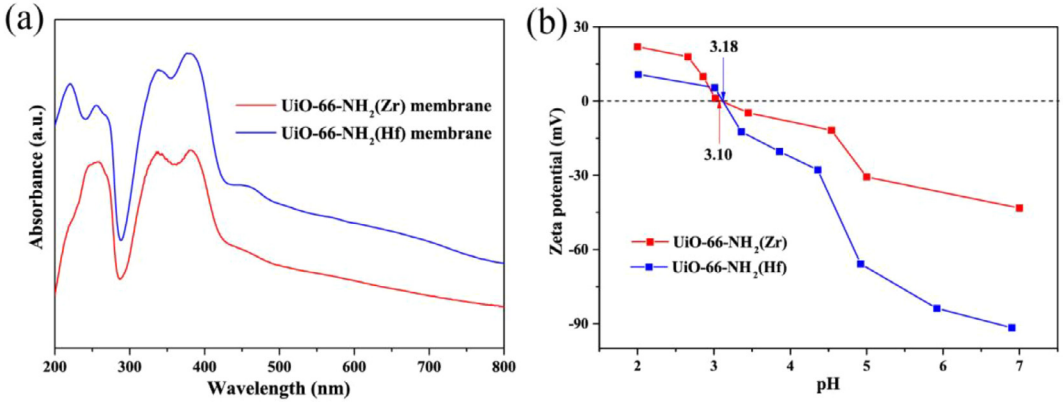

Fig. 3. (a) UV–vis spectra of UiO-66-NH_2(Zr/Hf) membranes. (b) Effect of pH on zeta potential of UiO-66-NH_2(Zr/Hf) in pure water system.

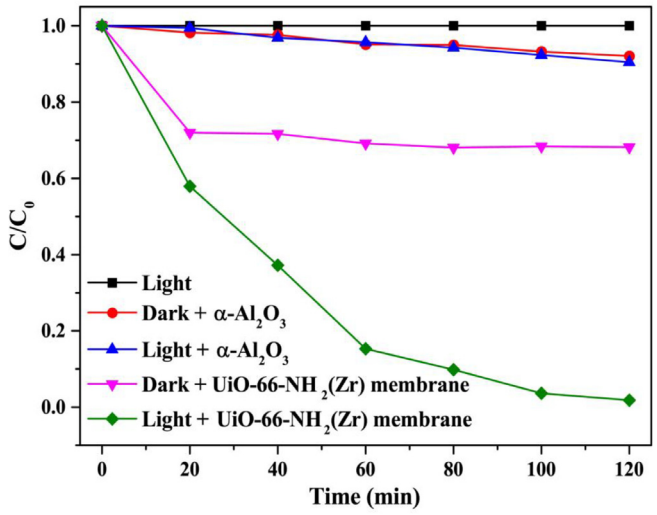

Fig. 4. The Cr(VI) removal profiles of UiO-66-NH_2(Zr) membrane under different conditions. Reaction conditions: no catalyst and α-Al_2O_3 support, α-Al_2O_3 support at dark, α-Al_2O_3 support at simulated sunlight irradiation, UiO-66-NH_2(Zr) membrane at dark, and UiO-66-NH_2(Zr) membrane at simulated sunlight irradiation.

The SEM images of the UiO-66-NH_2(Zr) membrane (Fig. 2d) and UiO-66-NH_2(Hf) membrane (Fig. S2a) revealed that their membrane surfaces are homogeneous and dense, with particle sizes of 300–500 nm, in which the surface microstructures of the UiO-66-NH_2(Zr/Hf) membrane are octahedrons resulting from the modulation via the addition of H_2Ac [29]. The thickness of the UiO-66-NH_2(Zr/Hf) membrane is ca. 8 μm determined by an ellipsometer, which is similar to the MIL-53(Al) membrane made by Yao and coworkers [27]. The loaded UiO-66-NH_2(Zr/Hf) is ca. 20.0 mg per α-Al_2O_3 support, which was determined from the mass difference value between the α-Al_2O_3 support and its supported UiO-66-NH_2(Zr/Hf) membrane.

Fig. 2e shows the PXRD pattern of the membranes. The characteristic peaks of the UiO-66-NH_2(Zr) and UiO-66-NH_2(Hf) crystals match well with the simulated diffraction patterns from single crystal structure data for UiO-66-NH_2(Zr/Hf) (CCDC 1405751). The two main feature peaks at 7.4° and 8.6° are assigned to their (1 1 1) and (0 0 2) reflections, respectively [30]. The FTIR spectra of powder separated from the surface of membrane is conducted to further identify the powder is UiO-66-NH_2(Zr). As shown in Fig. 2f, the absorption peaks at 1576 cm^{-1}, 1423 cm^{-1}, 1259 cm^{-1} and 669 cm^{-1} can be assigned to the stretching modes of C-O, C-C, C_{ar}-N and Zr/Hf-O, respectively, which matched perfectly with pristine UiO-66-NH_2(Zr/Hf) [31].

Optical absorption of the UiO-66-NH_2(Zr/Hf) MOF membranes was investigated by UV-vis DRS, as illustrated in Fig. 3a and Fig. S3. The broad peaks between 200 and 430 nm are consistent with the absorption of powder UiO-66-NH_2 [19]. However, the UiO-66-NH_2(Zr/Hf) MOF membranes pose a new absorption peak centered around 460 nm with a long tail on the longer wavelength side. The new peak at ~460 nm might originate from the metal to ligand charge transfer (MLCT) or d-d transition of the metals [32]. Considering that no 4d elections are in the Zr^{4+} and Hf^{4+} ions, it is reasonable to rule out the d-d transition in the MOF membranes, therefore the MLCT mainly contributes the new absorption peak in the visible region. Compared with UiO-66-NH_2 MOFs, the extended absorption in the visible region of the UiO-66-NH_2(Zr/Hf) MOF membranes could lead to enhanced

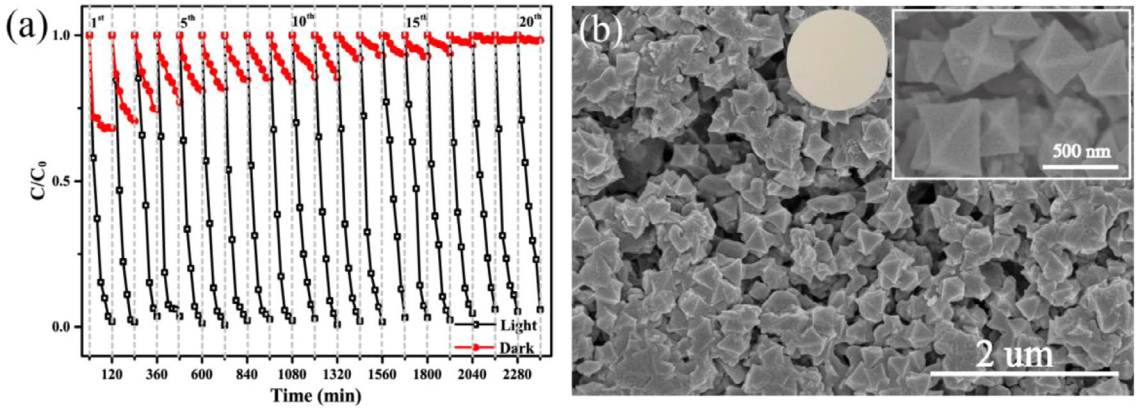

Fig. 5. (a) Reusability of UiO-66-NH_2(Zr) membrane under simulated sunlight irradiation (photocatalytic Cr(VI) reduction) and at dark conditions (adsorption toward $Cr_2O_7^{2-}$) for 20 successive cycles. (b) SEM of UiO-66-NH_2(Zr) membrane surface after the 20th photocatalysis experiment.

Table 1
Performance of some typical metal-organic frameworks as photocatalysts for the Cr(VI) reduction under visible light irradiation.

Photocatalyst/Amount (mg)	Cr(VI) solution Volume (mL)/ concentration (ppm)/pH	hole scavenger	Time/ (min)	1st run cycle Reduction efficiency (%)	Times/last run cycle Reduction efficiency (%)	Ref.
NH_2-MIL-125(Ti)/20	50/48/2.1	EtOH	60	97	5/90	[36]
UiO-66(NH_2)/20	40/10 /2.0	MeOH	80	97	3/97	[19,37]
NH_2–MIL-88B (Fe)/20	40 /8 /2.0	NA	50	100	4/100	[34]
MIL-101(Fe)/20	40/8/2.0	NA	60	100	NA	[34]
MIL-68(In)-NH_2/40	40 /20 /2.0	EtOH	180	97	3/97	[38]
MIL-53(Fe)/40	40/20/3.0	$(NH_4)_2C_2O_4$	40	100	5/100	[39]
$[Cu_2I_2(BPEA)](DMF)_4$/15	40/10/3.09	MeOH	9	95	3/95	[40]
NNU-36/15	40/10/2.17	MeOH	60	95.3	4/90	[16]
UiO-66-NH_2(Zr)/20	40/5/2.0	NA	120	98	20/94	This work

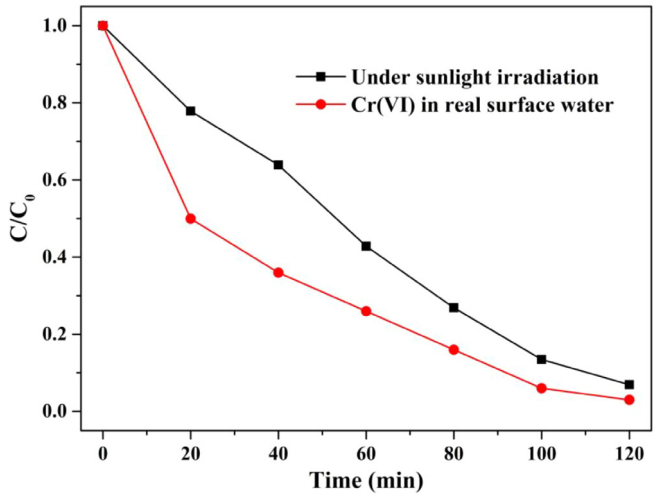

Fig. 6. Photocatalytic reduction performance toward Cr(VI) in ultra-pure water solution of UiO-66-NH_2(Zr) membrane under direct sunlight irradiation (luminous power 70 mW cm^{-2}) and toward Cr(VI) in real lake water solution under simulated sunlight irradiation (5.0 ppm Cr(VI), pH = 2.0).

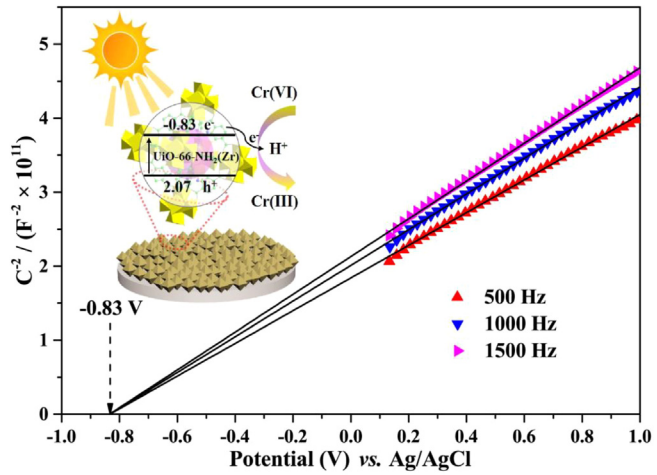

Fig. 7. The Mott–Schottky plot of UiO-66-NH_2(Zr) in 0.2 M Na_2SO_4 aqueous solution (pH = 6.8) and possible mechanism of photocatalytic reduction of Cr (VI) over UiO-66-NH_2(Zr) membrane (inset).

visible light photocatalytic activity on the target reactions.

3.2. Evaluation of photocatalytic activity

To assess the photocatalytic performances of the prepared UiO-66-NH_2(Zr/Hf) membranes, the Cr(VI) reduction efficiency at pH = 2 under simulated sunlight irradiation were measured. As shown in Fig. 4, control experiments without the UiO-66-NH_2(Zr) membrane photocatalyst and in absence of light leads to no reduction of Cr(VI) to Cr(III). The α-Al_2O_3 substrate possesses minor adsorption performance toward $Cr_2O_7^{2-}$ (ca. 10.0%), while both UiO-66-NH_2(Zr) membrane and UiO-66-NH_2(Hf) membrane exhibit a certain quantity of adsorption toward $Cr_2O_7^{2-}$ (ca. 30.0% for the former, and ca. 17.0% for the latter), resulting from their positive zeta potential values (+22 mV for the former, and +13 mV for the latter) at pH being 2.0 (Fig. 3b) [33]. Under the irradiation of simulated sunlight, both UiO-66-NH_2(Zr) and UiO-66-NH_2(Hf) membranes can rapidly reduce more than 98.0% Cr (VI) into Cr(III) within 120 min (Fig. 4 and S4), following Eqs. (1) and (2) [20,34]. The reduction efficiencies of Cr(VI) over UiO-66-NH_2(Zr) membrane at different pH values were shown in Fig. S5, in which the reduction ratio decreased rapidly with the pH increase (98.0%, 89.9%, and 62.0% at pH = 2, 4 and 6, respectively) [13].

$$Cr_2O_7^{2-} + 14H^+ + 6e^- \rightarrow 2Cr^{3+} + 7H_2O \quad (1)$$

$$2H_2\ O + 2h^+ \rightarrow H_2O_2 + 2H^+ \quad (2)$$

The photocatalysts in membrane form are easy to separate from treated aqueous Cr(VI) solution while also providing advantageously high stability and reusability [35]. It is essential to check the long-term stability of the membrane photocatalyst for practical application. In each recycle experiment, the membrane was only washed with deionized water and dried at 333 K for 6 h. As shown in Fig. 5a, the reduction efficiency of Cr(VI) to Cr(III) of the UiO-66-NH_2(Zr) membrane can be maintained up to 94.1% after twenty runs (2400 min). In addition, as shown in Fig. 5b, there is no significant change in the octahedron morphology of the UiO-66-NH_2(Zr) membrane after twenty runs, indicating the UiO-66-NH_2(Zr) membrane can be used repeatedly without obvious photocatalyst defect. However, starting from the tenth run, the reduction efficiency of Cr(VI) to Cr(III) over the UiO-66-NH_2(Hf) membrane gradually reduces to 70.0% after twenty runs (Fig. S6), which might result from the relatively poor affinity of UiO-66-NH_2(Hf) with α-Al_2O_3.

It should be noted that, compared to the powder form of the MOFs, the contact area ratio between UiO-66-NH_2(Zr) membrane and the Cr (VI) might decrease significantly, which could lead to the decrease of reaction rate and efficiencies. In this study, the reduction efficiency of Cr(VI) over UiO-66-NH_2(Zr) powder was also higher than that of UiO-66-NH_2(Zr) membrane (Fig. S7). However, we can achieve 94.0–98.0% Cr(VI) removal in 120 min for 20 runs under the condition of ca. 20 mg UiO-66-NH_2(Zr) in membrane form, 30 mL of 5 ppm Cr(VI) solution, pH = 2.0 without the addition of methanol as a hole scavenger to promote the reaction. This data is comparable with some of the results obtained with MOF powders, as illustrated in Table 1. For example, Wu and coworkers reported 97.0% Cr(VI) reduction in 80 min under the reaction conditions of 20 mg UiO-66-NH_2(Zr) powder, 40 mL of 10 ppm Cr(VI) solution, 100 μL methanol and pH = 2.0 [19]. The reduction efficiency of Cr(VI) over UiO-66-NH_2(Zr) membrane increased when the ethanol as hole scavenger was presented in the solution, as shown in Fig. S8. As well, the photocatalyst in the MOF membranes can facilitate

the reuse and recyclability of the photocatalyst.

Similarly, the photocatalytic Cr(VI) reduction experiments were conducted under direct sunlight irradiation in the presence of UiO-66-NH_2(Zr) membrane. All the experimental conditions were kept the same as the ones under the simulated sunlight irradiation except the source of irradiation. The sunlight experiment was carried out on a bright sunny day from 12 am to 2 pm of 1st, June 2018 at the location of BUCEA DaXing Campus (39°44′ N latitude and 116°17′ E longitude). The photocatalytic Cr(VI) reduction results under direct sunlight irradiation (Fig. 6) revealed that ca. 93.1% Cr(VI) was transformed into Cr(III) within 120 min, implying that UiO-66-NH_2(Zr) membrane can achieve efficient photocatalytic activity while exposed to real sunlight.

In order to elevate the influence of dissolved foreign ions toward photocatalytic Cr(VI) reduction activity, the real lake water (K^+, 4.5 mg/L; Na^+, 35.6 mg/L; Ca^{2+}, 67.4 mg/L; Mg^{2+}, 32.1 mg/L; Cl^-, 32.0 mg/L; NO_3^-, 11.8 mg/L; SO_4^{2-}, 174.1 mg/L; PO_4^{3-}, 0.4 mg/L; COD_{Mn}, 11.6 mg/L) sampled from the Ming Lake in BUCEA DaXing campus was used to prepare the Cr(VI) solution. As demonstrated in Fig. 6, the photocatalytic Cr(VI) reduction efficiency (97.0% within 120 min) was not inhibited by total salts in real lake water, indicating UiO-66-NH_2(Zr) membrane possessed the potential feasibility to conduct Cr(VI) reduction in real wastewater.

In this study, transient photocurrent responses under intermittent visible light irradiation and Mott-Schottky measurements were carried out to verify the electrochemical properties of UiO-66-NH_2(Zr) powder samples prepared under the identical conditions to the UiO-66-NH_2(Zr) membrane. The Mott-Schottky measurement results revealed that the positive slope of the obtained C^{-2}-E plot matches well with n-type photocatalyst, as shown in Fig. 7 and Fig. S10. The flat-band potentials of UiO-66-NH_2(Zr) and UiO-66-NH_2(Hf) are −0.83 V and −0.92 V *vs.* Ag/AgCl at pH = 6.8, respectively, which are more negative than the Cr (VI)/Cr(III) potential (+0.51 V, pH = 6.8; +1.15 V, pH = 3.0) [38]. The result of the transient photocurrent responses of UiO-66-NH_2(Zr/Hf) as illustrated in Fig. S9 indicated they are able to be photoexcited to generate electron-hole pairs under intermittent visible light irradiation. Thus, it is thermodynamically possible to transfer photogenerated electrons to achieve Cr(VI) reduction to Cr(III) over UiO-66-NH_2(Zr) membrane. The corresponding reaction processes can be described as Eqs. (1) and (3).

$$\text{UiO}-66-\text{NH}_2(\text{Zr}) + h\nu \rightarrow \text{UiO}-66-\text{NH}_2(\text{Zr})(e^- + h^+) \quad (3)$$

4. Conclusion

The UiO-66-NH_2(Zr/Hf) membranes were successfully fabricated on alumina porous supports by a facile reactive seeding method. The structure and morphology of the obtained metal-organic framework membranes were characterized by PXRD, FTIR, SEM, and UV-Vis DRS. And the UiO-66-NH_2(Zr/Hf) membrane showed an outstanding performance in the photocatalytic reduction of Cr(VI) under both simulated and real sunlight. After twenty runs, about 94.1% of Cr(VI) was still reduced and the crystal structure of UiO-66-NH_2(Zr) membrane was almost unaffected. Also, the presence of foreign ions, commonly found in water samples, in the solution posed no obvious inhabitation to the Cr(VI) reduction activities of the UiO-66-NH_2(Zr) membrane. Therefore, the UiO-66-NH_2(Zr/Hf) MOF membranes have great potential for the photocatalytic removal of pollutants from real wastewater because of their easy separation from treated solution and facile reuse without loss of photocatalyst efficiency, while avoiding the addition of organic hole scavenger reagents.

Acknowledgements

This work was supported by National Natural Science Foundation of China (51578034), Great Wall Scholars Training Program Project of Beijing Municipality Universities (CIT&TCD20180323), Project of Construction of Innovation Teams and Teacher Career Development for Universities and Colleges Under Beijing Municipality (IDHT20170508), Beijing Talent Project (2017A38), and the Fundamental Research Funds for Beijing Universities (X18075/X18076).

Appendix A. Supplementary data

Supplementary data to this article can be found online at https://doi.org/10.1016/j.cej.2018.09.084.

References

[1] R.J. Kieber, J.D.W. And, S.D. Zvalaren, Chromium Speciation in Rainwater: temporal variability and atmospheric deposition, Environ. Sci. Technol. 36 (2002) 5321–5327.
[2] J.J. Testa, M.A. Grela, M.I. Litter, Heterogeneous photocatalytic reduction of chromium(VI) over TiO_2 particles in the presence of oxalate: involvement of Cr(V) species, Environ. Sci. Technol. 38 (2004) 1589–1594.
[3] A.K. Bhattacharya, T.K. Naiya, S.N. Mandal, S.K. Das, Adsorption, kinetics and equilibrium studies on removal of Cr(VI) from aqueous solutions using different low-cost adsorbents, Chem. Eng. J. 137 (2008) 529–541.
[4] Arda Kabay, Streat, Removal of Cr(VI) by solvent impregnated resins (SIR) containing aliquat 336, React. Funct. Polym. 54 (2003) 103–115.
[5] U. Divrikli, A.A. Kartal, M. Soylak, L. Elci, Preconcentration of Pb(II), Cr(III), Cu(II), Ni(II) and Cd(II) ions in environmental samples by membrane filtration prior to their flame atomic absorption spectrometric determinations, J. Hazard. Mater. 145 (2007) 459–464.
[6] C.E. Barreradíaz, V. Lugolugo, B. Bilyeu, A review of chemical, electrochemical and biological methods for aqueous Cr(VI) reduction, J. Hazard. Mater. 223–224 (2012) 1–12.
[7] S. Park, W. Kim, R. Selvaraj, Y. Kim, Spontaneous reduction of Cr(VI) using $InSnS_2$ under dark condition, Chem. Eng. J. 321 (2017) 97–104.
[8] L.B. Khalil, W.E. Mourad, M.W. Rophael, Photocatalytic reduction of environmental pollutant Cr(VI) over some semiconductors under UV/visible light illumination, Appl. Catal. B: Environ. 17 (1998) 267–273.
[9] Y. Ku, I.L. Jung, Photocatalytic reduction of Cr(VI) in aqueous solutions by UV irradiation with the presence of titanium dioxide, Water Res. 35 (2001) 135–142.
[10] F. Zhang, Y. Zhang, G. Zhang, Z. Yang, D.D. Dionysiou, A. Zhu, Exceptional synergistic enhancement of the photocatalytic activity of SnS_2 by coupling with polyaniline and N-doped reduced graphene oxide, Appl. Catal. B: Environ. 236 (2018) 53–63.
[11] Z. Wu, X. Yuan, G. Zeng, L. Jiang, H. Zhong, Y. Xie, H. Wang, X. Chen, H. Wang, Highly efficient photocatalytic activity and mechanism of Yb^{3+}/Tm^{3+} codoped In_2S_3 from ultraviolet to near infrared light towards chromium(VI) reduction and rhodamine B oxydative degradation, Appl. Catal. B: Environ. 225 (2018) 8–21.
[12] W. Liu, W. Sun, A.G. Borthwick, T. Wang, F. Li, Y. Guan, Simultaneous removal of Cr(VI) and 4-chlorophenol through photocatalysis by a novel anatase/titanate nanosheet composite: Synergetic promotion effect and autosynchronous doping, J. Hazard. Mater. 317 (2016) 385–393.
[13] C.C. Wang, X.D. Du, J. Li, X.X. Guo, P. Wang, J. Zhang, Photocatalytic Cr(VI) reduction in metal-organic frameworks: a mini-review, Appl. Catal. B: Environ. 193 (2016) 198–216.
[14] H. Li, S. Yao, H.L. Wu, J.Y. Qu, Z.M. Zhang, T.B. Lu, W. Lin, E.B. Wang, Charge-regulated sequential adsorption of anionic catalysts and cationic photosensitizers into metal-organic frameworks enhances photocatalytic proton reduction, Appl. Catal. B: Environ. 224 (2018) 46–52.
[15] C.C. Wang, J.R. Li, X.L. Lv, Y.Q. Zhang, G. Guo, Photocatalytic organic pollutants degradation in metal–organic frameworks, Energy Environ. Sci. 7 (2014) 2831–2867.
[16] H. Zhao, Q. Xia, H. Xing, D. Chen, H. Wang, Construction of pillared-layer MOF as efficient visible-light photocatalysts for aqueous Cr(VI) reduction and dye degradation, ACS Sustain. Chem. Eng. 5 (2017) 4449–4456.
[17] R. Liang, F. Jing, L. Shen, N. Qin, L. Wu, MIL-53(Fe) as a highly efficient bifunctional photocatalyst for the simultaneous reduction of Cr(VI) and oxidation of dyes, J. Hazard. Mater. 287 (2015) 364–372.
[18] H. Kaur, M. Venkateswarulu, S. Kumar, V. Krishnan, R.R. Koner, A metal-organic framework based multifunctional catalytic platform for organic transformation and environmental remediation, Dalton. T. 47 (2018) 1488–1497.
[19] L. Shen, S. Liang, W. Wu, R. Liang, L. Wu, Multifunctional NH2-mediated zirconium metal-organic framework as an efficient visible-light-driven photocatalyst for selective oxidation of alcohols and reduction of aqueous Cr(VI), Dalton Trans. 42 (2013) 13649–13657.
[20] L. Shen, W. Wu, R. Liang, R. Lin, L. Wu, Highly dispersed palladium nanoparticles anchored on UiO-66(NH_2) metal-organic framework as a reusable and dual functional visible-light-driven photocatalyst, Nanoscale 5 (2013) 9374.
[21] S. Leong, A. Razmjou, K. Wang, K. Hapgood, X. Zhang, H. Wang, TiO_2 based photocatalytic membranes: a review, J. Membrane. Sci. 472 (2014) 167–184.
[22] J. Gascon, F. Kapteijn, Metal-Organic Framework Membranes-High Potential, Bright Future? Angew. Chem. Int. Edit. 49 (2010) 1530–1532.
[23] Y. Sun, F. Yang, Q. Wei, N. Wang, X. Qin, S. Zhang, B. Wang, Z. Nie, S. Ji, H. Yan, Oriented Nano–Microstructure-Assisted Controllable Fabrication of Metal-Organic Framework Membranes on Nickel Foam, Adv. Mater. 28 (2016) 2374–2381.

[24] Z.Q. Li, M. Zhang, B. Liu, C.Y. Guo, M. Zhou, Rapid fabrication of metal–organic framework thin films using in situ microwave irradiation and its photocatalytic property, Inorg. Chem. Comm. 36 (2013) 241–244.
[25] M. Kanezashi, K. Yada, T. Yoshioka, T. Tsuru, Design of silica networks for development of highly permeable hydrogen separation membranes with hydrothermal stability, J. Am. Chem. Soc. 131 (2009) 414–415.
[26] Q. Wei, F. Wang, Z.R. Nie, C.L. Song, Y.L. Wang, Q.Y. Li, Highly Hydrothermally Stable Microporous Silica Membranes for Hydrogen Separation, J. Phys. Chem. B 112 (2008) 9354–9359.
[27] Y. Hu, X. Dong, J. Nan, W. Jin, X. Ren, N. Xu, Y.M. Lee, Metal-organic framework membranes fabricated via reactive seeding, Chem. Comm. 47 (2010) 737–739.
[28] Y.C. Zhang, J. Li, M. Zhang, D.D. Dionysiou, Size-tunable hydrothermal synthesis of SnS_2 nanocrystals with high performance in visible light-driven photocatalytic reduction of aqueous Cr(VI), Environ. Sci. Technol. 45 (2011) 9324–9331.
[29] A. Schaate, P. Roy, A. Godt, J. Lippke, F. Waltz, M. Wiebcke, P. Behrens, Modulated synthesis of Zr-based metal-organic frameworks: from nano to single crystals, Chem. 17 (2011) 6643–6651.
[30] J. Starck, E. Toppila, I. Pyykko, Structural determination of a highly stable metal-organic framework with possible application to interim radioactive waste scavenging: Hf-UiO-66, Phys. Rev. B 86 (2012) 1514–1517.
[31] J. Yang, Y. Dai, X. Zhu, Z. Wang, Y. Li, Q. Zhuang, J. Shi, J. Gu, Metal-organic frameworks with inherent recognition sites for selective phosphate sensing through their coordination-induced fluorescence enhancement effect, J. Mater. Chem. A 3 (2015) 7445–7452.
[32] W. Zheng, K. Singh, Z. Wang, J.T. Wright, T.J. Van, N.S. Dalal, R.W. Meulenberg, G.F. Strouse, Evidence of a $ZnCr_2Se_4$ spinel inclusion at the core of a Cr-doped ZnSe quantum dot, J. Am. Chem. Soc. 134 (2012) 5577–5585.
[33] K. Wang, J. Gu, N. Yin, Efficient removal of Pb(II) and Cd(II) using NH_2-functionalized Zr-MOFs via rapid microwave-promoted synthesis, Ind. Eng. Chem. Res. 56 (2017) 1880–1887.
[34] L. Shi, T. Wang, H. Zhang, K. Chang, X. Meng, H. Liu, J. Ye, An amine-functionalized iron (III) metal–organic framework as efficient visible-light photocatalyst for Cr (VI) reduction, Adv. Sci. 2 (2015) 1500006.
[35] X. Liu, N.K. Demir, Z. Wu, K. Li, Highly Water-Stable Zirconium Metal-Organic Framework UiO-66 Membranes Supported on Alumina Hollow Fibers for Desalination, J. Am. Chem. Soc. 137 (2015) 6999–7002.
[36] H. Wang, X. Yuan, Y. Wu, G. Zeng, X. Chen, L. Leng, Z. Wu, L. Jiang, H. Li, Facile synthesis of amino-functionalized titanium metal-organic frameworks and their superior visible-light photocatalytic activity for Cr(VI) reduction, J. Hazard. Mater. 286 (2015) 187–194.
[37] L. Shen, R. Liang, M. Luo, F. Jing, L. Wu, Electronic effects of ligand substitution on metal-organic framework photocatalysts: the case study of UiO-66, Phys. Chem. Chem. Phys. 17 (2015) 117–121.
[38] R. Liang, L. Shen, F. Jing, W. Wu, Q. Na, L. Rui, W. Ling, NH_2 -mediated indium metal–organic framework as a novel visible-light-driven photocatalyst for reduction of the aqueous Cr(VI), Appl. Catal. B: Environ. 162 (2015) 245–251.
[39] R. Liang, F. Jing, L. Shen, N. Qin, L. Wu, MIL-53(Fe) as a highly efficient bifunctional photocatalyst for the simultaneous reduction of Cr (VI) and oxidation of dyes, J. Hazard. Mater. 287 (2015) 364–372.
[40] D.-M. Chen, C.-X. Sun, C.-S. Liu, M. Du, Stable Layered Semiconductive Cu (I)–Organic Framework for Efficient Visible-Light-Driven Cr(VI) Reduction and H_2 Evolution, Inorg. Chem. 57 (2018) 7975–7981.